Mechanism of the heavy-ion charge exchange reaction 12C(12C, 12N)12B at 35 MeV/nucleon

Winfield, J.S.; Anantaraman, N.; Austin, Sam M.; Harwood, L.H.; Plicht, J. van der; Zeller, A.F.

Published in:
Physical Review C

DOI:
10.1103/PhysRevC.33.1333

Publication date:
1986

Mechanism of the heavy-ion charge exchange reaction $^{12}C(^{12}C,^{12}N)^{12}B$ at 35 MeV/nucleon

J. S. Winfield, N. Anantaraman, Sam M. Austin, L. H. Harwood,
J. van der Plicht, H.-L. Wu, and A. F. Zeller
National Superconducting Cyclotron Laboratory and Department of Physics and Astronomy, Michigan State University, East Lansing, Michigan 48824
(Received 9 December 1985)

The heavy-ion charge exchange reaction $^{12}C(^{12}C,^{12}N)^{12}B$ has been studied at $E(^{12}C)=35$ MeV/nucleon. Angular distributions in the range 3.7–12.1° (c.m.) have been measured for the 1^+ (0.0 MeV), 2^+ (0.95 MeV), 2^- (1.67 MeV), and $4^-,2^-$ (4.5 MeV) states in ^{12}B. A broad peak at 7.8 MeV excitation was also observed. Microscopic one-step distorted-wave Born approximation calculations yield $V_{\sigma\tau}$ strengths ≥ 2 times those obtained in (p,n) reactions at similar energies per nucleon. Although this is significantly smaller than $V_{\sigma\tau}$ values obtained in other heavy-ion charge exchange studies, mostly carried out at energies less than 10 MeV/nucleon, it is concluded that the reaction mechanism is still dominated by sequential transfer (two-step) processes at 35 MeV/nucleon. A rough estimate indicates that one-step processes will dominate at bombarding energies above about 50 MeV/nucleon.

I. INTRODUCTION

Heavy-ion charge exchange reactions offer several potential advantages over (p,n) reactions as spectroscopic tools for the study of Gamow-Teller (GT) and other spin-dependent transitions in nuclei. Perhaps most important is the selectivity of the spin transfer channel for certain projectile-ejectile choices: for example, $(^{12}C,^{12}N)$ is a 0^+ to 1^+ transition and hence should selectively excite $\Delta S=\Delta T=1$ transitions. Heavy-ion charge exchange reactions also allow the equivalent of both (p,n) and (n,p) reactions, may facilitate the study of high spin states in the target nucleus, and provide for more exotic phenomena such as double charge exchange. Although charge exchange reactions induced by ^{6}Li have been widely studied (see, e.g., Refs. 1–3) and several studies of the $(^7Li,^7Be)$ reaction have been made,[4] only a few detailed investigations have been undertaken with heavier projectiles: these include $(^{12}C,^{12}B)$, $(^{13}C,^{13}B)$, $(^{13}C,^{13}N)$, $(^{18}O,^{18}F)$, $(^{48}Ti,^{48}Sc)$, and $(^{48}Ti,^{48}V)$ (Refs. 5–9).

A disadvantage of charge exchange reactions with low-energy heavy ions is that the one-step process, which is of most interest for spectroscopic studies, must compete with a large amplitude for the sequential transfer of nucleons (i.e., one nucleon pickup and stripping). Indeed, where detailed studies have been made of the reaction mechanism,[5,8] the two-step processes are found to dominate. However, these experiments were performed at beam energies of less than 10 MeV per nucleon, and since the sequential nucleon transfer is predicted to fall off exponentially with increasing beam energy,[10] one expects the one-step process to become dominant at sufficiently high energies. As a reference point, the (p,n) reaction at energies above 25 MeV appears to be well described by a one-step mechanism.[11]

We report here on the results of an exploratory experiment with ^{12}C projectiles at 35 MeV/nucleon. The reaction studied, $(^{12}C,^{12}N)$, would certainly be a useful, and perhaps a unique, spectroscopic probe of β^+ strength in nuclei if it proceeds through a one-step mechanism. It is probably easier experimentally than (n,p) and is more selective as regards spin transfer than lighter probes such as $(^7Li,^7Be)$ which allow both $\Delta S=0$ and $\Delta S=1$ transitions. The latter reaction has the additional complication that ^{7}Be in both its ground and first excited states will be present. This complication is absent in the present reaction, since ^{12}N has no particle-stable excited states.

In this paper we first present details of the experiment and a qualitative discussion of the data. One-step distorted-wave Born approximation (DWBA) calculations are then described. We show that the magnitudes of the predicted one-step cross sections are significantly smaller than the data and infer that other processes are more important, although the dominance of these other processes is not as great as observed at lower energies. A rough estimate indicates that the one-step process will dominate at energies above about 50 MeV/nucleon.

II. EXPERIMENTAL PROCEDURE

A 35 MeV/nucleon $^{12}C^{4+}$ beam from the K500 cyclotron at the National Superconducting Cyclotron Laboratory was used to bombard a 480 ± 30 μg/cm^2 ^{12}C target. The ^{12}N reaction products were momentum analyzed by the S-320 spectrograph,[12] which has a quadrupole-quadrupole-dipole-multipole configuration. The spectrograph aperture was 0.25 msr with a horizontal angular acceptance of $\pm0.3°$. Spectra were measured for laboratory angles between 1.75° and 5.75° in 1° steps. The focal plane detector consisted of two position-sensitive proportional counters, an ion chamber for ΔE information, and a plastic scintillator which provided both total energy information and a stop signal for time of flight relative to the cyclotron rf. Identification of the ^{12}N particles was achieved in a standard way through two-dimensional plots of the above parameters.

Relative normalizations for each angular setting of the spectrograph were based on counts in a monitor detector fixed at approximately 7° to the beam. This monitor detector consisted of a 3 mm thick plastic scintillator with an active area of 40 mm^2 connected via an optical fiber to an external phototube. The absolute normalization of the data was based on the integrated current measured in a Faraday cup located about 1.5 m from the target. Elastic scattering data for $^{12}C + ^{12}C$ at 420 MeV has previously been measured by Loveman[13] and an optical model potential derived. A check of our normalization procedure was therefore possible by comparing elastic scattering data taken during the present experiment for $\theta_{lab}=3.75°-8.75°$ with Loveman's results. Our data agreed with that work to within ±10%. The total normalization error in the present experiment is estimated at ±11%; this is not included in the error bars on the data shown in Sec. IV.

The focal plane of the spectrograph was calibrated by measuring the centroids of the peaks corresponding to elastic scattering and inelastic scattering to the 2^+, 4.44 MeV state in ^{12}C for five different magnet settings. These calibration points were fitted by a second-order polynomial.

III. QUALITATIVE DISCUSSION OF THE DATA

Sample spectra for $^{12}C(^{12}C,^{12}N)^{12}B$ are displayed in Fig. 1. The energy resolution of the peaks corresponding to discrete states in ^{12}B is 700 keV FWHM. The very broad feature in the 1.8° spectrum, labeled by the symbol H, arises from the reaction on hydrogen in the target; at the larger observed angles the $^1H(^{12}C,^{12}N)n$ reaction is kinematically forbidden.

The most prominent feature in all the spectra is the peak at 4.5 MeV which corresponds to the unresolved 4^- (4.52 MeV) and 2^- (4.46 MeV) states in ^{12}B. The strength of the peak compared to that of the low-lying levels and the angular momentum mismatch for the reaction ($\sim 4.5\hbar$) suggests that most of the contribution is from the higher spin state; this agrees with our determination of the peak energy, 4.55±0.03 MeV. Strong population of states near 4.5 MeV has also been observed in the $^{12}C(d,^2He)^{12}B$ reaction[14] and in the mirror nucleus ^{12}N by von Oertzen *et al.*[6]

Among several broad peaks at higher excitation, one centered at 7.8 MeV excitation in ^{12}B is of interest. A similar feature has been observed by von Oertzen *et al.*[6] in both $^{12}C(^{13}C,^{13}B)^{12}N$ and $^{12}C(^{13}C,^{13}N)^{12}B$, and it corresponds to the analog of the giant dipole resonance (GDR) in ^{12}C. We note that the reactions ($^{13}C,^{13}B$), ($^{13}C,^{13}N$), and (n,p) (Ref. 15) all excite the GDR analog strongly, while the $\Delta S=1$ reactions (d,^{2}He) (Ref. 14) and ($^{12}C,^{12}N$) (this work) do so only weakly, presumably because the GDR excitation is largely non-spin-flip. In general, the ($^{13}C,^{13}N$) and ($^{13}C,^{13}B$) reactions[6] seem much less $\Delta S=1$ selective than the reaction studied here: the 2^+ ($\Delta S=0$ allowed) excitation dominates the spectrum for ($^{13}C,^{13}N$) and is stronger than the ground state ($1^+,\Delta S=1$) transition for ($^{13}C,^{13}B$).

Angular distributions have been extracted for the peak at 4.5 MeV, the ground state, and the first two excited states. A Gaussian peak-fitting program was used to extract yields for the latter states. The fitting procedure was to fix the centroids at the predicted positions for the first iteration, and then allow them to vary. Consistent peak positions were obtained for all angles.

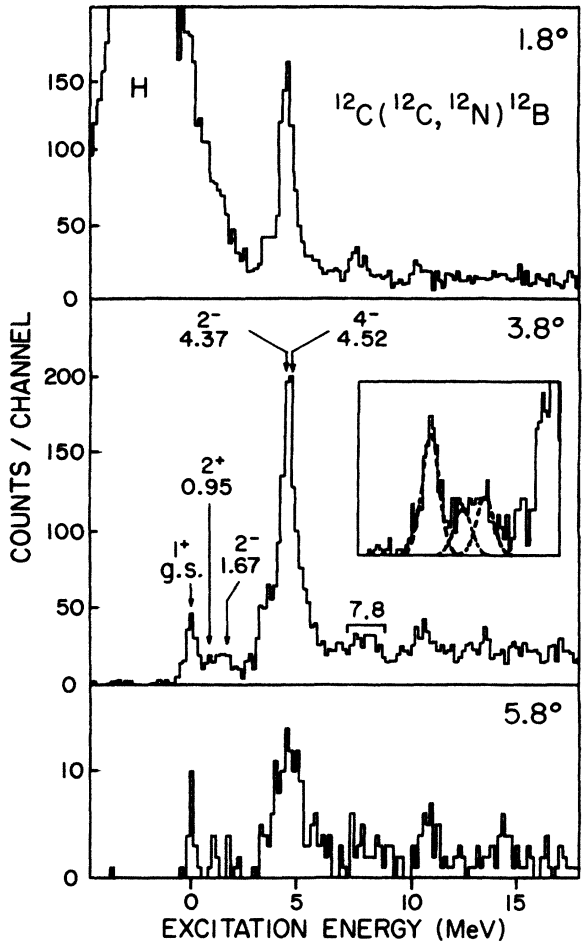

FIG. 1. Spectra for $^{12}C(^{12}C,^{12}N)^{12}B$ at 35 MeV/nucleon. The spectrograph angle (laboratory) is indicated for each case. The symbol H indicates background from the $^1H(^{12}C,^{12}N)n$ reaction. The insert in the 3.8° spectrum shows overlaid on the data the unfolded Gaussian peaks from the fitting procedure for the lowest three levels of ^{12}B.

IV. RESULTS OF MICROSCOPIC DWBA ANALYSIS

Microscopic DWBA calculations have been performed for comparison with the four experimental angular distributions extracted (Fig. 2). Charge exchange form factors calculated with the code described by Etchegoyen *et al.*[5] were used in the distorted wave code MARS (Ref. 16). The form factor calculation directly uses shell-model one-body transition amplitudes for the target and projectile systems. For example, in the target-residual (A-B) system:

$$\mathrm{OBTD}(AB\rho\rho';j,t)=\frac{\langle I_B T_B|||(a_\rho^\dagger\times\tilde{a}_{\rho'})^{j,t}|||I_A T_A\rangle}{\sqrt{(2j+1)(2t+1)}}, \quad (1)$$

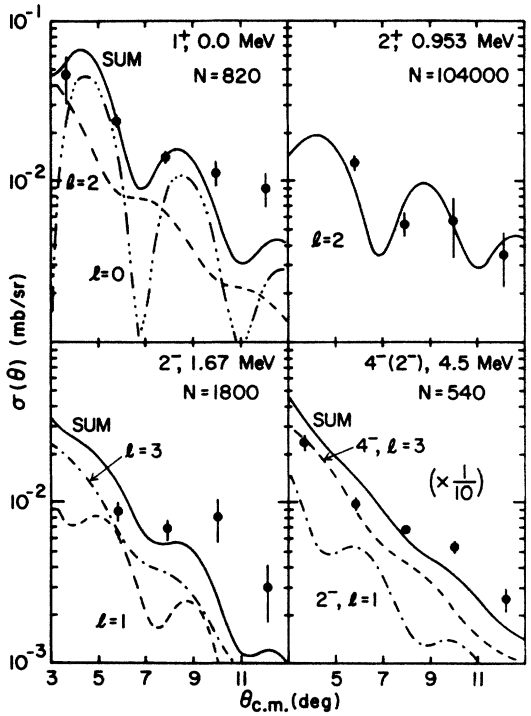

FIG. 2. Angular distributions for the transitions to the states at $E_x=0.0$ (1^+), 0.953 (2^+), 1.67 (2^-), and 4.5 (4^-,2^-) MeV in ^{12}B. The curves are one-step DWBA calculations multiplied by a factor of N as shown.

as defined in Ref. 17. Here j and t are the total angular momentum and isospin transferred to the target system. These amplitudes were calculated with the code OXBASH (Ref. 18) and are listed in Table I. We also list values of the coefficients $C_{\rho\rho'}$ as defined in Refs. 5 and 8 in terms of multinucleon transition densities, $g^{lsj;t}$.

For the 1^+ and 2^+ states the model space was restricted to the p shell; for the 2^- state the entire *spsd* shells were included with the restrictions of no more than one particle in the *sd* shell and no more than one 0*s* hole. The 4^- state is the so-called "stretched" state with a $0d_{5/2}0p_{3/2}^{-1}$ configuration.

Since the spins and parities of ^{12}C and ^{12}N impose $\Delta S=1$ if a one-step mechanism is assumed, the only part of the central nucleon-nucleon interaction required in the form factor is the $V_{\sigma\tau}$ component. The tensor and exchange terms were not included; the effects of neglecting these will be discussed below. The form of the interaction used was a single Yukawa,

$$v(r_{ij})=V_{\sigma\tau}\exp(-\mu r_{ij})/(\mu r_{ij}) ,$$

where r_{ij} is the separation between the two interacting nucleons and μ is the inverse range parameter, set to 1.0 fm^{-1} in the present work.

Bound state radial wave functions were generated from a Woods-Saxon potential with geometrical parameters $R=1.25A_T^{1/3}$ fm and $a=0.65$ fm, and a spin orbit well depth of 7 MeV. For the particle-stable bound states, the depth of the central potential was adjusted so that the eigenenergy matched the experimental separation energies

TABLE I. Coefficients of one body transitions densities (OBTD) of Eq. (1) and values of $C_{\rho\rho'}$ [the $C_{\rho\rho'}$ are defined in Refs. 5 and 8, but note that the OBTD given in Ref. 5 correspond to the ones given here divided by $\sqrt{(2I_B+1)(2T_B+1)}$]. The following two-body interactions were used: Cohen-Kurath (Ref. 19) (*p* shell); Millener-Kurath (Ref. 20) (1p-1h and 0*s* shell); and Preedom-Wildenthal (Ref. 21) (*sd* shell). Here l_1 is the orbital angular momentum transferred to the intrinsic motion of the target system.

(i) ^{12}C→^{12}N[1^+] g.s. and ^{12}C→^{12}B[1^+] g.s.

Initial	Final	OBTD	$C_{\rho\rho'}(l_1=0)$	$C_{\rho\rho'}(l_1=2)$
$p_{1/2}$	$p_{1/2}$	−0.0581	0.0109	−0.0309
$p_{3/2}$	$p_{1/2}$	−0.6902	−0.3671	−0.1298
$p_{1/2}$	$p_{3/2}$	−0.3394	0.1805	0.0638
$p_{3/2}$	$p_{3/2}$	−0.0764	−0.0454	0.0128

(ii) ^{12}C→^{12}B[2^+] 0.95 MeV

Initial	Final	OBTD	$C_{\rho\rho'}(l_1=2)$
$p_{3/2}$	$p_{1/2}$	0.6801	0.2972
$p_{1/2}$	$p_{3/2}$	−0.1132	0.0495
$p_{3/2}$	$p_{3/2}$	0.0608	0.0000

(iii) ^{12}C→^{12}B[2^-] 1.67 MeV.

Initial	Final	OBTD	$C_{\rho\rho'}(l_1=1)$	$C_{\rho\rho'}(l_1=3)$
$0s_{1/2}$	$p_{3/2}$	0.0086	0.0048	0.0000
$p_{1/2}$	$d_{3/2}$	−0.0307	0.0035	−0.0470
$p_{3/2}$	$d_{3/2}$	0.0142	0.0032	0.0039
$p_{1/2}$	$d_{5/2}$	0.0076	−0.0042	−0.0009
$p_{3/2}$	$d_{5/2}$	0.3577	0.1849	−0.0431
$p_{3/2}$	$1s_{1/2}$	−0.6945	−0.3918	0.0000

(iv) ^{12}C→^{12}B[2^-] 4.46 MeV

Initial	Final	OBTD	$C_{\rho\rho'}(l_1=1)$	$C_{\rho\rho'}(l_1=3)$
$0s_{1/2}$	$p_{3/2}$	−0.0061	−0.0034	0.0000
$p_{1/2}$	$d_{3/2}$	−0.0723	0.0082	−0.0400
$p_{3/2}$	$d_{3/2}$	−0.0911	−0.0206	−0.0252
$p_{1/2}$	$d_{5/2}$	−0.3228	0.1784	0.0364
$p_{3/2}$	$d_{5/2}$	0.5419	0.2802	−0.0654
$p_{3/2}$	$1s_{1/2}$	0.3315	0.1870	0.0000

(v) ^{12}C→^{12}B[4^-] 4.52 MeV

Initial	Final	OBTD	$C_{\rho\rho'}(l_1=3)$
$p_{3/2}$	$d_{5/2}$	−0.8034	−0.5140

of the relevant nucleon in ^{12}C, ^{12}N, and ^{12}B. The 2^- (4.46 MeV) and 4^- (4.52 MeV) states in ^{12}B are unbound with respect to neutron emission ($S_n=3.37$ MeV). For these states the "weak binding" approximation in which the neutron is assumed to be bound by 100 keV was used. Since this approximation is somewhat suspect[22] for heavy ions, we estimated the error it introduces by repeating the 4^- calculation using the method of complex-energy eigenstates [calculated with the code GAMOV4 (Ref. 22)] for the $d_{5/2}$ neutron wave function in ^{12}B. The magnitude of the cross section calculated with the complex eigenstate method was found to be 40% lower than that with the

TABLE II. Optical model potentials from $^{12}C + ^{12}C$ elastic scattering.

V (MeV)	W (MeV)	r_v^a (fm)	r_w^a (fm)	a_v (fm)	a_w (fm)	E/A^b (MeV)	E_{DW}/A^c (MeV)	Ref.
180	56.7	0.69	0.89	0.79	0.73	30	35	23
180	600	0.735	0.408	0.75	0.85	25	25	24
250	193.6	0.456	0.959	0.994	0.470	35	45–55	13
11	25	1.35	1.27	0.5	0.25	3–10[d]	5–10	25
200	68	0.70	0.96	0.87	0.69	24	15	26

[a] $R_x = r_x(A_T^{1/3} + A_P^{1/3})$.
[b] Energy/nucleon at which the potential was determined from elastic scattering.
[c] This column indicates which potentials were used for a given bombarding energy (in MeV/nucleon) for the DWBA calculations of the energy dependence of σ_{1step} and σ_{seq}.
[d] An approximate potential which does not fit both forward and backward angle scattering data simultaneously. See original reference for details.

weak binding approximation. This leads to a 20% higher value for $V_{\sigma\tau}$. The shapes of the angular distributions were similar in both cases.

For the results presented here, the optical potential for both entrance and exit channels was set "G" of Buenerd *et al.*[23] which fitted 360 MeV $^{12}C + ^{12}C$ elastic scattering data. A rather different potential—especially in terms of the depth of the imaginary potential—from the analysis by Bohlen *et al.*[24] of 300 MeV $^{12}C + ^{12}C$ scattering data, gave a very similar shape for the angular distribution but the cross sections were approximately 35% smaller. The potential from Loveman,[13] which should describe the entrance channel correctly, gave slightly poorer fits to the data and cross sections approximately 25% higher than those from the first potential. The three potentials are listed in Table II.

One hundred partial waves were used in the distorted wave calculations. The difference between cross sections calculated using 90 and 100 partial waves was less than one percent. Although the distorted wave code we used does not account for the indistinguishability of the particles in the entrance channel, it is believed that this would be a small correction for the angular range under consideration ($\theta < 13°$ c.m.). The differential cross section is steeply falling and the magnitude of $\sigma(\pi - \theta)$ is negligible compared with $\sigma(\theta)$ at these angles. For comparison, elastic scattering calculations with and without antisymmetrization of the projectile and target amplitudes performed with the code ECIS79 (Ref. 27) show less than 0.1% difference in the cross section out to 26° (c.m.).

The calculated angular distributions for the one-step process are shown in Fig. 2 together with the normalization factors required to fit the data. For the 2^- (4.46 MeV) and 4^- (4.52 MeV) calculations the lower of the two possible L transfers gives the larger contribution to the total cross section (by an order of magnitude), and the higher L transfer angular distribution is omitted from the figures for clarity. This is not the case for the 1^+ ground state, where the $\Delta L = 2$ part dampens the oscillations from the $\Delta L = 0$ cross section, and for the 2^- (1.67 MeV)

TABLE III. Values of $V_{\sigma\tau}$ strengths required to fit charge exchange data in one-step calculations for a Yukawa interaction with range 1.0 fm.

Reaction	E/A (MeV)	J_f	$V_{\sigma\tau}$ (MeV)	Ref.
$^{12}C(^{12}C,^{12}N)^{12}B$	35	1^+	29	a
	35	2^+	320	a
	35	2^-	42	a
	35	$4^-(2^-)$	23	a
(p,n), (p,p'); $A = 6$–26	25–50	various	11.7±1.7	28
$^{25,26}Mg(^6Li,^6He)$	6	various	22–33[b]	29
$(^6Li,^6He)$; $A = 18$–48	6	1^+	22–28	30
	6	$3^+,5^+,7^+$	20–250	30
$^{28}Si(^{18}O,^{18}F)^{28}Al$	3	$3^+(2^+)$	76	8
$^{26}Mg(^{12}C,^{12}B)^{26}Al$	9	$5^+,3^+$	120,170	5

[a] Present work.
[b] $V_{\sigma\tau} \approx 17$ (16) MeV when exchange (+ tensor) forces included.

state, where the higher L-transfer contribution is actually slightly greater than that from the lower L transfer owing to the magnitude of the respective form factors (i.e., the nuclear structure). It is also noted that for the states at 4.5 MeV the DWBA predicts a 4^- (4.52 MeV) cross section more than twice that for the 2^- (4.46 MeV) state, as expected from the kinematic matching of the reaction.

Although the angular extent of the data is rather limited, the one-step DWBA gives a fair representation of the data in terms of the general shape of the angular distribution. A more critical test of the model lies in the extracted value of the strength of the interaction, $V_{\sigma\tau}$ (the computer code assumes $V_{\sigma\tau}=1$ MeV, so the value necessary to fit the data would be the square root of the cross section normalization factor). The strengths of $V_{\sigma\tau}$ required to fit the data are given in Table III together with results from other charge exchange reactions. The most accurate determination of $V_{\sigma\tau}$ in this energy range is probably the average value of 11.7 ± 1.7 MeV obtained from a variety of (p,n) and (p,p') studies.[28] While it is true that the values of $V_{\sigma\tau}$ obtained here for (^{12}C,^{12}N) (with the notable exception of the transition to the 2^+ state of ^{12}B) are smaller than values obtained previously for projectiles with $A>6$ (but at lower energy), there is still a large discrepancy with the accepted value of $V_{\sigma\tau}$. For $V_{\sigma\tau}\approx12$ MeV, one-step calculations yield cross sections almost an order of magnitude smaller than the data (in the case of the 2^+ state, nearly three orders of magnitude smaller).

One might consider that the one-step DWBA cross sections presented here are overestimated, since many calculated (p,n) cross sections must be quenched by about 0.6 in order to agree with the observed strengths (see, e.g., Ref. 31). In Ref. 28, most calculations used to deduce the mean $V_{\sigma\tau}$ of 12 MeV were normalized to agree with the related matrix elements. Our shell model wave functions for $^{12}\mathrm{C}\rightarrow{}^{12}\mathrm{B}_{\mathrm{g.s.}}$ and $^{12}\mathrm{C}\rightarrow{}^{12}\mathrm{N}_{\mathrm{g.s.}}$ yield a $B(GT)$ value of 0.923 compared with 0.942 ± 0.006 from β decay.[32] Thus, at least for the ^{12}B ground state, we should not renormalize our cross sections.

V. DISCUSSION

A. Tensor force and exchange effects

Two contributions to the one-step reaction process have not been taken into account: one arising from the nucleon-nucleon tensor force and the other from antisymmetrization or exchange effects. The tensor force is believed to have little effect on charge exchange cross sections, except possibly at large momentum (q) transfer.[28] Gaarde *et al.*[33] found that the tensor force made a small contribution to unnatural parity, high spin states: for example, in the ^{48}Ca(^{6}Li,^{6}He)^{48}Sc (5^+) reaction, the cross section was decreased by 20%. For other states the contribution was negligible. Thus the neglect of the tensor force is unlikely to affect our conclusions.

On the other hand, exchange effects may play a significant role in certain charge exchange reactions, especially for transitions with large orbital angular momentum transfers. No calculations have been made for projectiles heavier than lithium, but we may estimate the magnitude of the effect from a study by Ciangaru *et al.*[29] of the (^{6}Li,^{6}He) reaction on magnesium targets. When single nucleon knockout exchange was included in their DWBA calculations, they found a reduction in $V_{\sigma\tau}$ of up to 50% for $\Delta L=4\hbar$ and of about 30% for $\Delta L\leq2\hbar$. The shape of the angular distribution was not significantly affected.

In view of the above considerations, it seems improbable that the major part of the discrepancy between the values of $V_{\sigma\tau}$ obtained in the present work and that obtained from nucleon-induced reactions could be removed if tensor or exchange effects were included, particularly for the case of the transition to the ground state of ^{12}B in which only low ΔL values are present. This implies that more complicated processes (e.g., sequential transfer of nucleons) continue to dominate over the one-step mechanism at beam energies as high as 35 MeV/nucleon. In regard to the very large value of $V_{\sigma\tau}$ for the 2^+ state, (which is the only natural-parity state studied here), one may conclude either that the observed cross section arises from processes other than one-step or that the wave function for this state is especially deficient.

B. Estimate of energy at which the one-step mechanism dominates

We have seen from the values of $V_{\sigma\tau}$ in Table III that the ^{12}C(^{12}C,^{12}N)^{12}B reaction at 35 MeV/nucleon is less dominated by two-step processes than other heavy-ion reactions (with $A>6$) at significantly lower bombarding energies, and we now estimate how high an energy is required before the reaction is primarily one-step. By performing a series of one-step DWBA calculations at different energies for ^{12}C(^{12}C,^{12}N)^{12}B, we have predicted the trend of the angle-integrated cross section in the range 10—60 MeV/nucleon (Fig. 3). In these calculations, appropriate optical potentials from $^{12}\mathrm{C}+{}^{12}\mathrm{C}$ scattering were selected from the literature for each energy (see Table II for details) and a $V_{\sigma\tau}$ strength of 12 MeV was used. The cross section rises exponentially until saturation is reached at about 40 MeV/nucleon (the scatter about the smooth curve is presumably due to the different

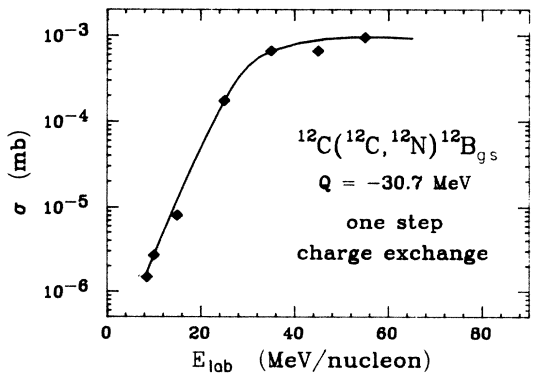

FIG. 3. Dependence of the one-step charge exchange cross section on incident energy. The points are results of DWBA calculations described in the text. The line is to guide the eye.

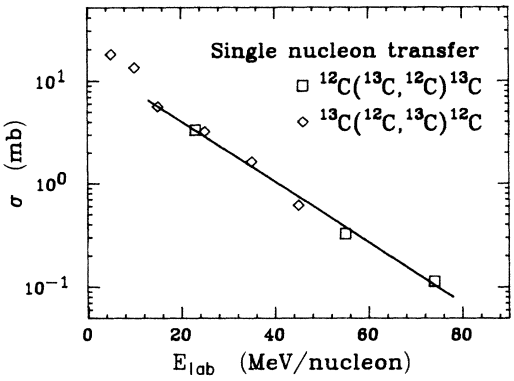

FIG. 4. Dependence of the single nucleon transfer reactions $^{13}C(^{12}C,^{13}C)^{12}C_{g.s.}$ and $^{12}C(^{13}C,^{12}C)^{13}C_{g.s.}$ on incident energy. The points are results of DWBA calculations. Diamonds: present work; squares: from Ref. 6. The line is to guide the eye.

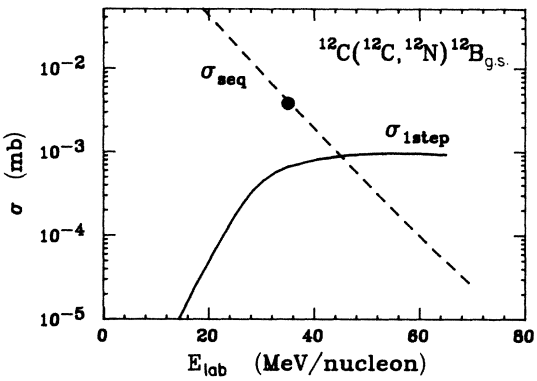

FIG. 5. Estimated trends of σ_{seq} and σ_{1step} with incident energy. The solid line (σ_{1step}) is taken from Fig. 3, the dashed line (σ_{seq}) is calculated from Eq. (2) and Fig. 4. The point represents the experimentally observed cross section for $^{12}C(^{12}C,^{12}N)^{12}B_{g.s.}$ at 35 MeV/nucleon.

optical model potentials used).

The lack of a heavy-ion coupled-reaction-channel code led us to make a rather crude approximation in order to estimate the trend of the sequential transfer cross section σ_{seq}, namely that

$$\sigma_{seq} \approx \frac{A\sigma_1\sigma_2}{\sqrt{E}} \approx \frac{A'(\sigma_1)^2}{\sqrt{E}} , \quad (2)$$

where σ_1 and σ_2 are the cross sections for single nucleon transfer and A and A' are constants. The inverse square root dependence on the energy is an approximation for the Green's function which mediates the propagation in the intermediate channel. The justification for this assumption comes from the two-step cross section for (p,n) charge exchange involving inelastic scattering:[34]

$$\sigma_{2step} \approx \frac{C}{\sqrt{E}} \sigma_{ch\,ex}\sigma_{inel} ,$$

where $\sigma_{ch\,ex}$ and σ_{inel} denote the individual charge exchange and inelastic scattering cross sections, respectively; the form of the two-step cross section for pickup and stripping is expected to be similar.[34] We have calculated the angle-integrated cross sections for the single nucleon transfer reaction $^{13}C(^{12}C,^{13}C)^{12}C_{g.s.}$ at various energies with the finite-range DWBA code SATURN-MARS (Ref. 16). Again a selection of optical model potentials was used from Table II. The cross sections are plotted in Fig. 4 along with similar predictions for the cross sections of $^{12}C(^{13}C,^{12}C)^{13}C_{g.s.}$ from von Oertzen.[6] As expected from considerations of the momentum transfer and recoil in heavy-ion reactions,[10,35] the cross section for single nucleon transfer decreases exponentially as the energy of the projectile is increased.

Finally, following Eq. (2) and Fig. 4 we plot the trend of σ_{seq} in Fig. 5, with the normalization determined by assuming that our measured $^{12}C(^{12}C,^{12}N)^{12}B$ cross section at 35 MeV/nucleon is essentially all sequential transfer and thus may be plotted as a point above the one-step prediction by $(29/12)^2$, i.e., the ratio of values of $(V_{\sigma\tau})^2$ from this paper (the 1^+ ground state transition is taken to be the most reliable) and the "best estimate" from Ref. 28. From Fig. 5 we estimate that the sequential transfer process becomes negligible at about 60 MeV/nucleon. This limit may be reduced to 50 MeV/nucleon if exchange effects increase the predicted one-step cross section by 30%.

VI. SUMMARY

In summary, we have measured angular distributions for the heavy-ion charge exchange reaction ($^{12}C,^{12}N$) on a ^{12}C target at significantly higher beam energies than in previous work and compared them with one-step DWBA calculations. Although the predicted cross sections are closer to experiment than for data at lower energy, it appears that other processes involving the sequential transfer of nucleons continue to predominate at 35 MeV/nucleon. A rough estimate indicates that the one-step mechanism does not become the most important process until a beam energy of about 50 MeV/nucleon is reached.

ACKNOWLEDGMENTS

We are grateful to L. Ray for providing a copy of the complex eigenstate code. We would like to thank M. Buenerd and A. Etchegoyen for helpful discussions and W. von Oertzen for a communication. This work was supported in part by the National Science Foundation under Grant No. PHY83-12245.

[1]W. R. Wharton, C. D. Goodman, and D. C. Hensley, Phys. Rev. C 22, 1138 (1980).

[2]A. Cunsolo, A. Foti, G. Imme, G. Pappalardo, G. Raciti, N. Saunier, and B. T. Kim, Nucl. Phys. A355, 261 (1981).

[3]D. V. Aleksandrov et al., Nucl. Phys. A436, 338 (1985).

[4]M. E. Williams-Norton, F. Petrovich, K. W. Kemper, R. J. Puigh, D. Stanley, and A. F. Zeller, Nucl. Phys. A313, 477 (1979); A. C. Dodd, N. M. Clarke, J. Coopersmith, R. J. Grif-

fiths, K. I. Pearce, B. Stanley, and J. Cook, J. Phys. G **11**, 1035 (1985); and references therein.

[5]A. Etchegoyen, D. Sinclair, S. Liu, M. C. Etchegoyen, D. K. Scott, and D. L. Hendrie, Nucl. Phys. **A397**, 343 (1983).

[6]W. von Oertzen, Lecture Notes of the Erice Summer School, 1984 (Interscience, New York, to be published); in *Frontiers in Nuclear Dynamics,* edited by R. A. Broglia and C. H. Dasso (Plenum, New York, 1985); W. von Oertzen *et al.*, Hahn-Meitner-Institut für Kernforschung, Berlin, Annual Report, 1984, p. 53.

[7]H. G. Bohlen, E. R. Flynn, A. Miczaika, and W. von Oertzen, in Abstracts of Contributed papers, International Symposium on Highly Excited States and Nuclear Structure, Orsay, edited by N. Marty and N. van Giai, 1983, p. 76 (unpublished).

[8]B. T. Kim, A. Greiner, M. A. G. Fernandes, N. Lisbona, K. S. Low, and M. C. Mermaz, Phys. Rev. C **20**, 1396 (1979).

[9]C. Brendel *et al.*, Proceedings of the 4th International Conference on Nuclei Far From Stability, Helsingør, 1981, CERN Report No. 81-09, p. 664.

[10]W. von Oertzen, Phys. Lett. **151B**, 95 (1985).

[11]W. A. Sterrenburg, Sam M. Austin, U. E. P. Berg, and R. P. DeVito, Phys. Lett. **91B**, 337 (1980).

[12]B. Sherrill, Ph.D. thesis, Michigan State University, 1984.

[13]R. A. Loveman, Ph.D. thesis, University of Washington, 1984.

[14]D. P. Stahel, R. Jahn, G. J. Wozniak, and J. Cerny, Phys. Rev. C **20**, 1680 (1979); K. B. Beard, J. Kasagi, E. Kashy, B. H. Wildenthal, D. L. Friesel, H. Nann, and R. E. Warner, *ibid.* **26**, 720 (1982).

[15]F. P. Brady *et al.*, J. Phys. G **10**, 363 (1984).

[16]T. Tamura and K. S. Low, Comp. Phys. Commun. **8**, 349 (1974).

[17]B. H. Wildenthal, in *Progress in Particle and Nuclear Physics,* edited by D. H. Wilkinson (Pergamon, New York, 1984), Vol. II, p. 5.

[18]W. D. M. Rae, A. Etchegoyen, N. S. Godwin, and B. A. Brown, shell model code OXBASH, Michigan State University Cyclotron Laboratory Report No. 524, 1983.

[19]S. Cohen and D. Kurath, Nucl. Phys. **73**, 1 (1976).

[20]D. J. Millener and D. Kurath, Nucl. Phys. **A255**, 315 (1975).

[21]B. M. Preedom and B. H. Wildenthal, Phys. Rev. C **6**, 1633 (1972).

[22]L. Ray, W. R. Coker, and T. Udagawa, Phys. Lett. **56B**, 318 (1975).

[23]M. Buenerd, A. Lounis, J. Chauvin, D. Lebrun, P. Martin, G. Duhamel, J. C. Gondrand, and P. de Saintignon, Nucl. Phys. **A424**, 313 (1984).

[24]H. G. Bohlen, M. R. Clover, G. Ingold, H. Lettau, and W. von Oertzen, Z. Phys. A **308**, 121 (1982).

[25]R. G. Stokstad *et al.*, Phys. Rev. C **20**, 655 (1979).

[26]M. E. Brandan, Phys. Rev. Lett. **49**, 1132 (1982).

[27]J. Raynal, computer code ECIS79, CEN-Saclay, 1979.

[28]S. M. Austin, in *The (p,n) reaction and the N-N force,* edited by C. D. Goodman *et al.* (Plenum, New York, 1980).

[29]G. Ciangaru, R. L. McGrath, and F. E. Cecil, Phys. Lett. **61B**, 25 (1976).

[30]W. R. Wharton and P. T. Debevec, Phys. Rev. C **11**, 1963 (1975).

[31]C. D. Goodman and S. D. Bloom, in *Spin Excitations in Nuclei,* edited by F. Petrovich *et al.* (Plenum, New York, 1984).

[32]C. D. Goodman, C. A. Goulding, M. B. Greenfield, J. Rapaport, D. E. Bainum, C. C. Foster, W. G. Love, and F. Petrovich, Phys. Rev. Lett. **44**, 1755 (1980).

[33]C. Gaarde, T. Kammuri, and F. Osterfeld, Nucl. Phys. **A222**, 579 (1974).

[34]V. A. Madsen and V. R. Brown, in *The (p,n) reaction and the N-N force,* edited by C. D. Goodman *et al.* (Plenum, New York, 1980).

[35]N. Anyas-Weiss *et al.*, Phys. Rep. **12C**, 203 (1974).